Proceedings of the 2023 International Conference on Mathematical Physics and Computational Simulation
DOI: 10.54254/2753-8818/28/20230428

Optimization of asymmetry of Pb-Pb nucleus collision based on Glauber model simulation

Haotian Xu[1,4, †], Junzhe Shi[2, †], Ziyan Song[3, †]

[1]Liberal Art College, University of Wisconsin–Madison, Wisconsin, 53706, USA
[2]Wuhan Britain-China School, Wuhan, 430010, China
[3]Guangdong Experimental High School, Guangzhou, 510380, China

[4]hxu393@wisc.edu
[†]These authors contributed equally to this work and should be considered co-first authors.

Abstract. Currently, researchers wanted to optimize the radiation by selecting certain asymmetry to produce high-energy particles in QGP collision. Our research utilized the Glauber-Monto-Carlo Model to simulate the collision and tried to find the domain of different independent variables to maximize the asymmetry of the cross-section. We have conducted relevant analysis and research on the principles of this model and generated relevant images using ROOT. The result shows that at the number level of 106, for the number of bins equals 10, we have (0.4, 0.5) for eccentricity in the second harmonic, (0.9, 1.0) for eccentricity in the third harmonic, (2.51, 3.14) for azimuthal angle difference, and (125, 166) for the number of participants, and, for number of bins equal to 20, (0.45, 0.50) for eccentricity in second harmonic, (0.95, 1.0) for eccentricity in the third harmonic, (2.82, 3.14) for azimuthal angle difference, and (146, 166) for the number of participants.

Keywords: Glauber Dynamics, Monto-Carlo Method, Asymmetry, Nucleus Collision**.**

1. Introduction

Since the first hardon particle collider was constructed in 1959 by CERN, people's research on particle science has never ceased. As one of the most prominent research methods, collisions between particles were predominant among most scientists. Through the collision of particles, researchers would be able to reveal the particle of different subatomic atoms. Notably, the nucleus, as one of the subatomic structures, was definitely one of them.

The nucleus, as the most passive component of the nucleus, was important for studies in various fields. From previous research from known scientists, we learned about the structure of protons and neutrons and the interactive force behind them. One of the most prominent theories would be CPT violation and unification of electric and weak interactive force [1-3]. While CPT violation opened the gates for research on the movements of particles in super-symmetry [4], the unification of electric and weak interactive force was considered a great step toward the theory of everything. As research progressed, scientists increased their knowledge of humanity about subatomic structures. Simulation of the distribution and dynamics in subatomic models turns out to be one of these fields.

DOI: 10.54254/2753-8818/28/20230428

In 1963, Roy Glauber in his paper introduced the methodology of Glauber dynamics. Starting from Ising Model, Dr. Glauber set the spins of particles in terms of -1 and 1. The exact value of spins was determined through a stochastic function based on time as the spins of one particle depend on the others due to the effect of heat [5]. The model used a discrete Markoff process to simulate the distribution pattern [6].

The Markoff process is a randomization process. Assuming exist two lists or variables, for which exists any xi belongs to space i is a natural number smaller than n and, ti < t, we have and only have xi = X(ti), which indicates no other functions in these two datasets deciding the value of one another. If these premises were fulfilled, we would have

$$P\{X(t) \leq x | x_i = X(t_i), 1 \leq i \leq n, i \subseteq Z\} = P\{X(t) \leq x | x_n = X(t_n)\} \tag{1}$$

For a process that fulfills the above condition, scientists called it the Markoff process. The research used a discrete Markoff process, meaning that the data points fulfill two properties, for which the probability of each plot is bigger than or equal to zero, and the summation of all probability would equal one. Therefore, Dr. Glauber used the discrete Markoff process, for which

$$P\{X(t) = x | x_i = X(t_i), 1 \leq i \leq n, i \subseteq Z\} = P\{X(t) = x | x_n = X(t_n)\} \tag{2}$$

Concerning the Markoff process, Dr. Glauber took the stopping time of the randomization process as the time t. After the simulation, Dr. Glauber first started with a single spin system and solved for the probability based on its spin and possibility based on time through a differential equation and substitute the probability based on time with the expectation value of the spin, which result in a form of

$$q(t) = q_o e^{-\alpha t} \tag{3}$$

$$p(\sigma, t) = \frac{1}{2[1 + \sigma q(t)]} \tag{4}$$

for which alpha is the double the rate of time particle's spin transit. Afterward, Dr. Glauber applied this to higher dimensions of spins and used the Markoff process with these given properties. Ultimately, Dr. Glauber solved the average spin for different systems. Using Glauber dynamics, Dr. Glauber developed a model in order to stimulate the nucleus collision.

Recently, there were researchers focused on searching for the emission rate of quark-gluon plasma (QGP) [7]. Researchers at McGill University studied the thermal radiation of photons in the transition stage from heavy hadrons to QGP [8]. As an outcome of their research, they found that the emission rate was based on relativistic emission, which was applicable for relativistic ion collision using multi-body calculation of lepton pairs. One of the interesting observations is the substantial effect of baryons on the emission of the spectrum. Baryons refer to particles composed of quarks and gluons. Therefore, through the Glauber model, we will be able to predict the emission of the spectrum based on the nucleus, as protons and neutrons are a class of baryons.

Currently, researchers devoted themselves to the particles produced during the collision of QGP. At a high energy level collision in QGP, scientists expected to discover traces of J/psi meson, phi meson, high momentum leptons, and strange hadrons. Throughout the studying of these particles, scientists would be able to study the bound state of the quark, quark association, and properties of QGP. Therefore, this created the importance to research on the methodology to produce the highest energy collision. On the other hand, currently, there were theories indicating the association between the spectrum radiation and asymmetry of the nucleus of the collision. As a result, we wanted to find the largest asymmetry of the nucleus producing the highest level of spectrum, which would indicate a high-energy collision.

2. Method

In our research, we chose to use Glauber Model for the simulation of the nucleus collision. Glauber Model, which was developed based on Glauber Dynamics, simulated this collision as an inelastic collision. The Glauber Model used Glauber Dynamics to set the wave function of the particles for the

DOI: 10.54254/2753-8818/28/20230428

collision and combined with the Fermi distribution in Gaussian form [9, 10]. The exact distribution is given in following for:

$$\rho(r) = \rho_0 \frac{1 + (\frac{w}{R})^2}{1 + \exp{(\frac{r^2 - R^2}{a^2})}} \tag{5}$$

where w, a, and R are special parameters. In our research, we used R = 6.62, w = 0, and a =0.546 since we used Pb as the element. ρo refers to the nucleon density, which was found during the process of running the Glauber Model. Deuteron and sulfur were two exceptions in this step of the simulation, which would perform differently with their probability distribution. However, since we particularly selected Pb as the elements during the collision, this difference in the model could temporarily be neglected. Professor Glauber introduced the Monto-Carlo method to describe the change in the status of the nucleus. For the changes, if the change in the spin leads to a decrease in energy, the change is automatically accepted. If the change in the spin leads to an increase in energy, the change would be determined through the probability of the quantum state at that point.

The collision process in Glauber Model was an inelastic collision, which was modeled through a function of energy [9]. Glauber Model named the collided particles as participants or wounded particles and the rest as the observers. The cross sections of the participants were given by the loss in energy, since the collision was an inelastic collision, indicating a loss in energy. This was the base where we could correlate the asymmetry of the cross-section with the energy radiated. Therefore, by simulating the collision in the Glauber model, we could find the cross-section with the highest symmetry to optimize the energy radiated.

In our research, we selected lead as the research subject. Compared to other elements, lead would be easier to create QGP due to higher luminosity compared to the light elements, and was easier to accelerate compared to heavy elements. Combing both factors, lead was currently the most variable element to research. Besides, there was already much research done on the performance of lead in the Large Hardon Collider (LHC). As a result, this would be helpful in correlating this research.

3. Analysis

After generating data from the simulation, we wanted to find the highest asymmetry with different variables. To measure asymmetry, we used the long radii of the cross-section and minus the short radii of the cross-section as one of the assumptions in the Glauber Model is the eclipse form of the cross-section. We selected the eccentricity of the second and third harmonic, the difference of angle between two azimuthal angles of two nuclei, and the number of participants. The selection of the above variables was based on two main reasons. Firstly, these variables were easy to manipulate in reality. Secondly, they were mostly directly related to the shape of the nucleus and the cross-section of collided parts of the nucleus. We could get this information by running the Glauber Model.

For the selection of the region, we chose zero to one for both eccentricities due to the mathematical definition of eccentricity. We chose 416 for the maximum number of participants because the largest stable isotope for lead was Pb-208. Since the collision required two particles, we multiplied 208 by 2 as the maximum. For the angles, we chose 2π for maximum, since this was the maximum value for any value according to the mathematical definition of radian and angle.

For extraction of the path length difference, we added a loop to determine the number of particles on the x and y axis assuming that the long axis and short axis are on the x and y axis. Therefore, counting the number of particles inside the region of (-0.5,0.5) for both the x and y axis would give us the length of this axis. Subsequently, by subtracting the long axis from the short axis, we would be able to obtain the path length difference.

Afterward, we chose to find the average number of the path length difference across a certain region over the independent variable. By correlating each data point on an independent variable to a path length difference, this would form two arrays containing two sets of points. Eventually, we summed the path length difference corresponding to points inside this region and divided it by the number of plots inside

DOI: 10.54254/2753-8818/28/20230428

this region. We chose to use a region instead of a particular data point due to the uncertainty principle. Based on the value of their independent variables, we could put them into a selected number of bins. Since we had four independent variables, we chose the following formula to calculate the average number

$$\Delta x_{average} = \frac{\Delta x_{total}}{n_{total}} = \frac{1}{n}\sum \Delta x \tag{6}$$

Δx here refers to all path length differences corresponding to selected independent variables, and n total here refers to the summation of the number of all selected independent variables. We established a loop comparing the value of the average path length differences. By storing the highest value as a temporary value, we discard the smallest path length difference and only store the largest difference. If there's any case where there are two same path length differences, the exact number would be shown and stored. After we generated our results, we generated a profile histogram for two independent variables and set the other two independent variables as constant, whose value is the same as the optimized value, to check the accuracy of the result.

4. Result

From our research, we concluded that the highest path length difference is 4.470864 fm, where the standard deviation is 0.036383 fm. Table 1 shows the domain of these independent variables.

Table 1. Relatively rough domain definitions of different variables [Owner-draw].

Independent Variable	Domain
Eccentricity at second harmonic	0.400 to 0.500
Eccentricity at third harmonic	0.900 to 1.000
Azimuthal angle difference	2.51 to 3.14
Number of Participants	125 to 166

These data were available at a level of 106 or above. The data at a lower sample size might lose their precision. For trials at the level of 6*105 to 7*105, the precision still remained. However, due to the smaller sample size, there was still room for more verification at this level. Besides, the precision would drop dramatically when it reached the level of 1*105. It totally fails accuracy when the sample size was below this level. This observation matches the Law of Big Numbers, which indicates that as the sample size increases, the mean value of the sample would be closer to the expected value. For twenty bins, we found a similar result. This trial was more precise than the ten-bin trials. Table 2 shows the result of this trial.

Table 2. Relatively precise domain definitions of different variables [Owner-draw].

Independent Variable	Domain
Eccentricity at the second harmonic	0.400 to 0.450
Eccentricity at the third harmonic	0.950 to 1.000
Azimuthal angle difference	2.82 to 3.14
Number of Participants	146 to 166

We found that the result of this trial was inside the domain of the first trial. This verified that the result we received for the first trial was consistent throughout our simulation. These trials were run at the level of 106 and turn out to produce similar results. These results matched the profile histograms, which turned out to be accurate (profile diagrams were shown and discussed in the graph section). The result from these graphs showed that the pathlength difference for the domain above was highest among all bars, proving that they had the largest pathlength difference among all domains.

DOI: 10.54254/2753-8818/28/20230428

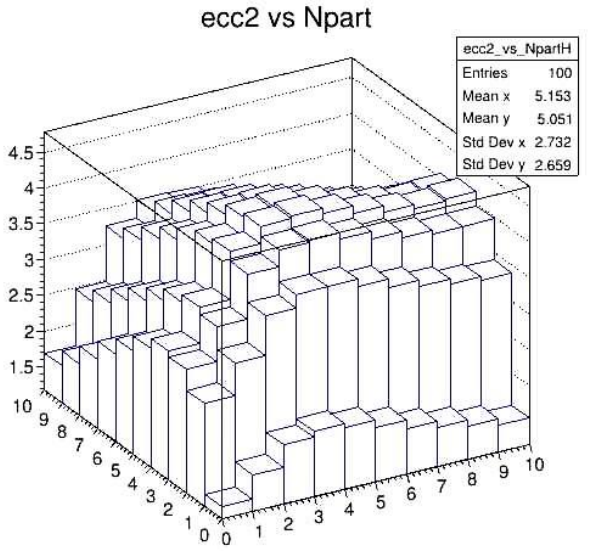

Figure 1. Domains for eccentricity in second harmonic and number of participants for ten bins [Owner-draw].

Figure 1 was generated by ROOT. Ecc2 refers to the eccentricity on second harmonic, while Npart refers to number of participants. x and y axis is ecc2 and Npart, while z axis is average pathlength difference for each bin and the unit of average path length difference is fm. It shows the domains for eccentricity in second harmonic and number of participants for ten bins. The value of azimuthal angle difference and eccentricity in third harmonic is set to the value in tenth bin and fifth bin, with index 9 and 4.

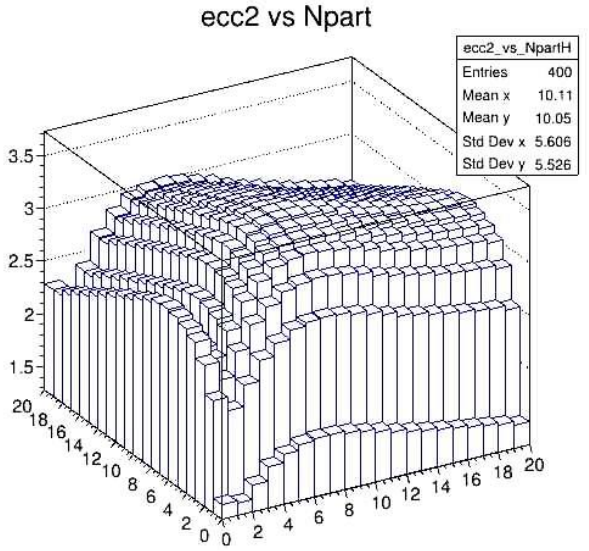

Figure 2. Domains for eccentricity in second harmonic and number of participants for twenty bins [Owner-draw].

Figure 2 was generated by ROOT. Ecc2 refers to the eccentricity on second harmonic, while Npart refers to number of participants. x and y axis is ecc2 and Npart, while z axis is average pathlength difference for each bin and the unit of average path length difference is fm. It shows the domains for eccentricity in second harmonic and number of participants for twenty bins. The value of azimuthal

DOI: 10.54254/2753-8818/28/20230428

angle difference and eccentricity in third harmonic is set to the value in twentieth bin and ten bin, with index 19 and 9.

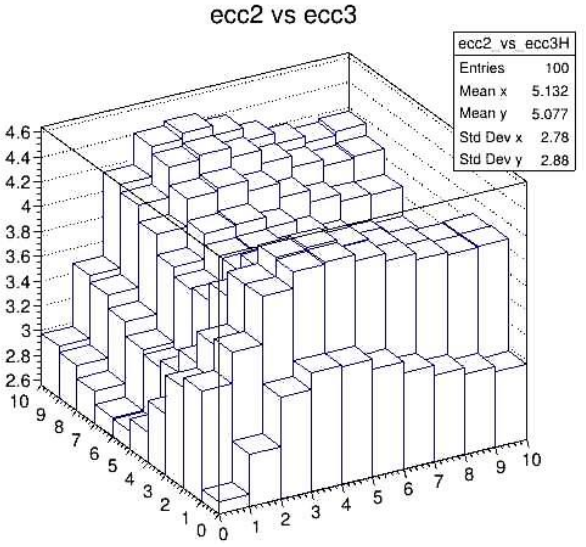

Figure 3. Domains for eccentricity in second harmonic and third harmonic for ten bins [Owner-draw].

Figure 3 was generated by ROOT. Ecc2 and ecc3 refers to the eccentricity on second and third harmonic. X and y axis is ecc2 and ecc3, while z axis is average pathlength difference for each bin and the unit of average path length difference is fm. It shows the domains for eccentricity in second harmonic and third harmonic for ten bins. The value of azimuthal angle difference and number of participants is set to the value in fifth bin and fourth bin, with index 4 and 3.

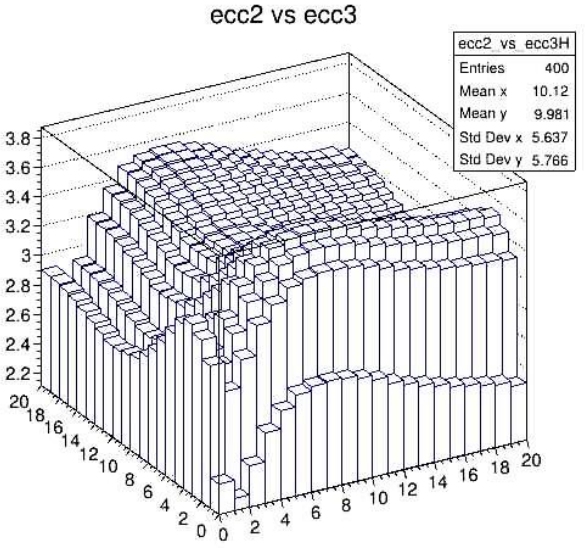

Figure 4. Domains for eccentricity in second harmonic and third harmonic for twenty bins [Owner-draw].

Figure 4 was generated by ROOT. Ecc2 and ecc3 refers to the eccentricity on second and third harmonic. X and y axis is ecc2 and ecc3, while z axis is average pathlength difference for each bin and the unit of average path length difference is fm. It shows the domains for eccentricity in second harmonic and third harmonic for twenty bins. The value of azimuthal angle difference and number of participants is set to the value in tenth bin and eighth bin, with index 9 and 7.

DOI: 10.54254/2753-8818/28/20230428

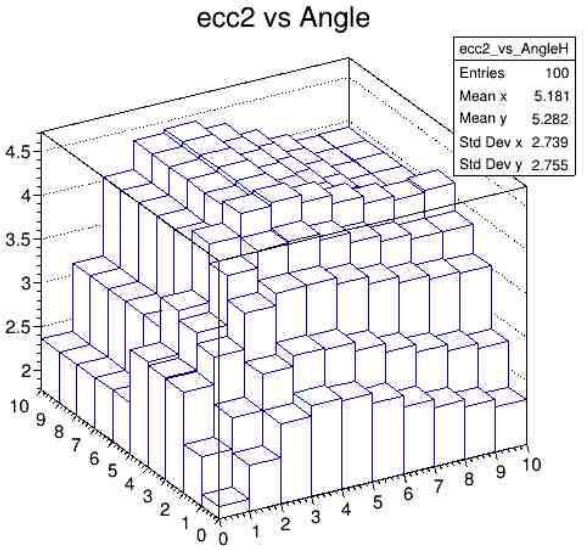

Figure 5. Domains for eccentricity in second harmonic and azimuthal angle difference for ten bins [Owner-draw].

Figure 5 was generated by ROOT. Ecc2 refers to the eccentricity on the second harmonic, while angle refers to the azimuthal angle difference. X and y axis are ecc2 and angle, while z-axis is the average pathlength difference for each bin and the unit of average path length difference is fm. It shows the domains for eccentricity in the second harmonic and azimuthal angle difference for ten bins. The value of eccentricity in the third harmonic and the number of participants is set to the value in the tenth bin and fourth bin, with indexes 9 and 3.

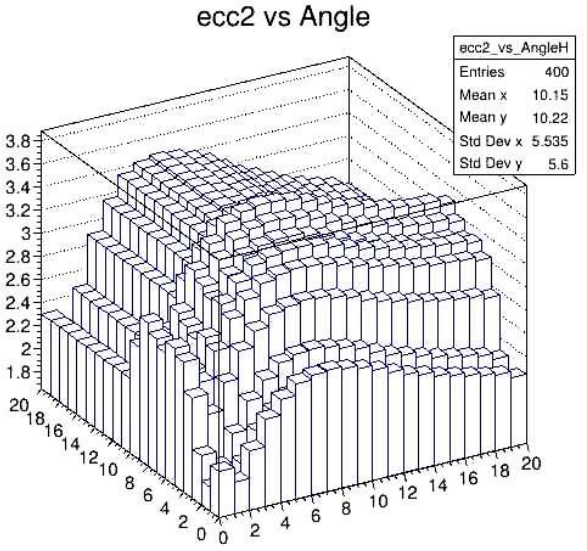

Figure 6. Domains for eccentricity in second harmonic and azimuthal angle difference for twenty bins [Owner-draw].

Figure 6 was generated by ROOT. Ecc2 refers to the eccentricity on second harmonic, while angle refers to azimuthal angle difference. X and y axis is ecc2 and angle, while z axis is average pathlength difference for each bin and the unit of average path length difference is fm. It shows the domains for eccentricity in second harmonic and azimuthal angle difference for twenty bins. The value of eccentricity

DOI: 10.54254/2753-8818/28/20230428

in third harmonic and number of participants is set to the value in tenth bin and fourth bin, with index 19 and 7.

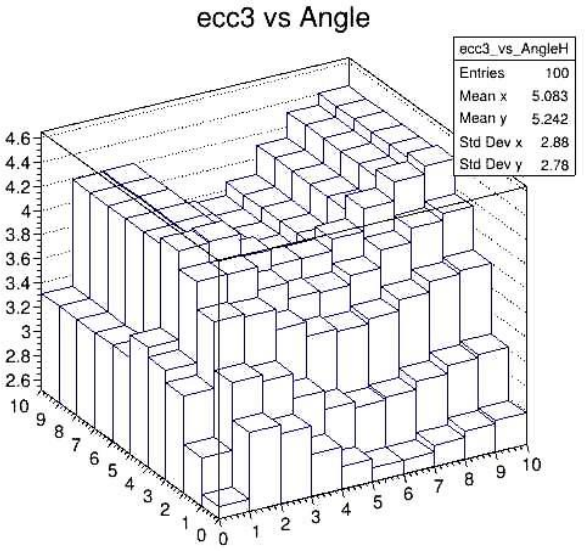

Figure 7. Domains for eccentricity in third harmonic and azimuthal angle difference for ten bins [Owner-draw].

Figure 7 was generated by ROOT. Ecc3 refers to the eccentricity on the third harmonic, while angle refers to the azimuthal angle difference. X and y axis is ecc3 and angle, while z axis is average pathlength difference for each bin and the unit of average path length difference is fm. It shows the domains for eccentricity in third harmonic and azimuthal angle difference for ten bins. The value of eccentricity in second harmonic and number of participants is set to the value in fifth bin and fourth bin, with index 4 and 3.

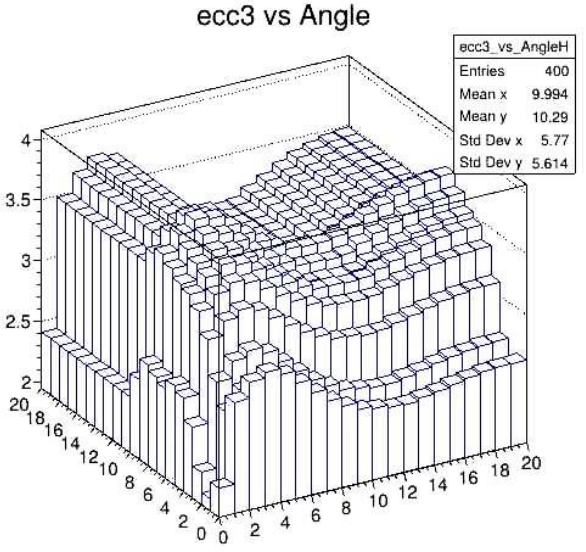

Figure 8. Domains for eccentricity in third harmonic and azimuthal angle difference for twenty bins [Owner-draw].

Figure 8 was generated by ROOT. Ecc3 refers to the eccentricity on third harmonic, while angle refers to azimuthal angle difference. X and y axis is ecc3 and angle, while z axis is average pathlength

DOI: 10.54254/2753-8818/28/20230428

difference for each bin and the unit of average path length difference is fm. It shows the domains for eccentricity in third harmonic and azimuthal angle difference for twenty bins. The value of eccentricity in second harmonic and number of participants is set to the value in ninth bin and eighth bin, with index 8 and 7.

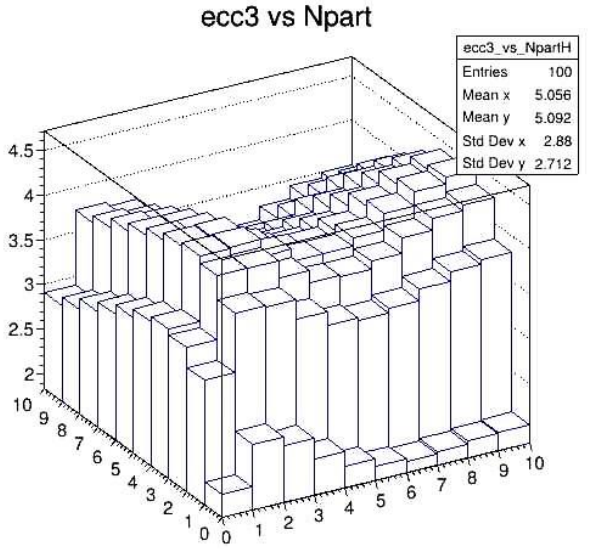

Figure 9. Domains for eccentricity in third harmonic and number of participants for ten bins [Owner-draw].

Figure 9 was generated by ROOT. Ecc3 refers to the eccentricity on third harmonic, while Npart refers to number of participants. x and y axis is ecc3 and Npart, while z axis is average pathlength difference for each bin and the unit of average path length difference is fm. It shows the domains for eccentricity in third harmonic and number of participants for ten bins. The value of eccentricity in second harmonic and azimuthal angle difference is set to the value in fifth bin, with index 4.

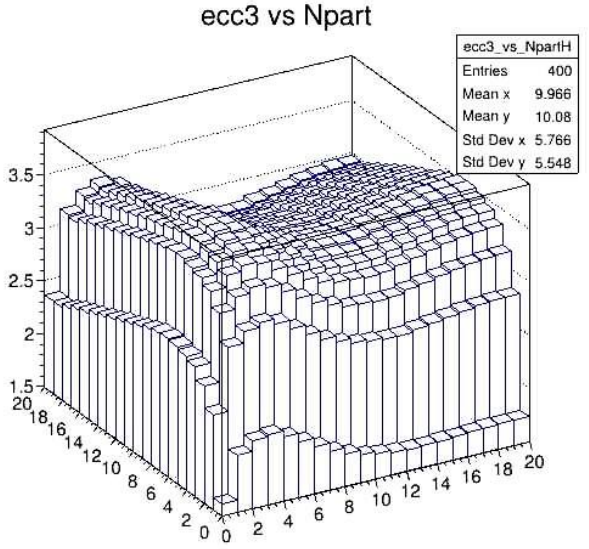

Figure 10. Domains for eccentricity in third harmonic and number of participants for twenty bins [Owner-draw].

DOI: 10.54254/2753-8818/28/20230428

Figure 10 was generated by ROOT. Ecc3 refers to the eccentricity on third harmonic, while Npart refers to number of participants. x and y axis is ecc3 and Npart, while z axis is average pathlength difference for each bin and the unit of average path length difference is fm. It shows the domains for eccentricity in third harmonic and number of participants for twenty bins. The value of eccentricity in the second harmonic and azimuthal angle difference is set to the value in ninth bin and tenth bin, with index 8 and 9.

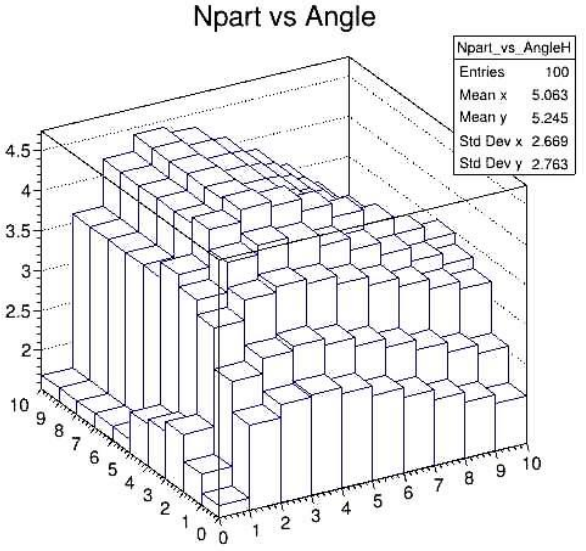

Figure 11. Domains for the number of participants and azimuthal angle difference for ten bins [Owner-draw].

Figure 11 was generated by ROOT. Npart refers to a number of participants, while angle refers to the azimuthal angle difference. x and y axis is Npart and angle, while z axis is the average path length difference for each bin and the unit of average path length difference is fm. It shows the domains for a number of participants and the azimuthal angle difference for ten bins. The value of eccentricity in second harmonic and third harmonics is set to the value in the fifth bin and tenth bin, with indexes 4 and 9.

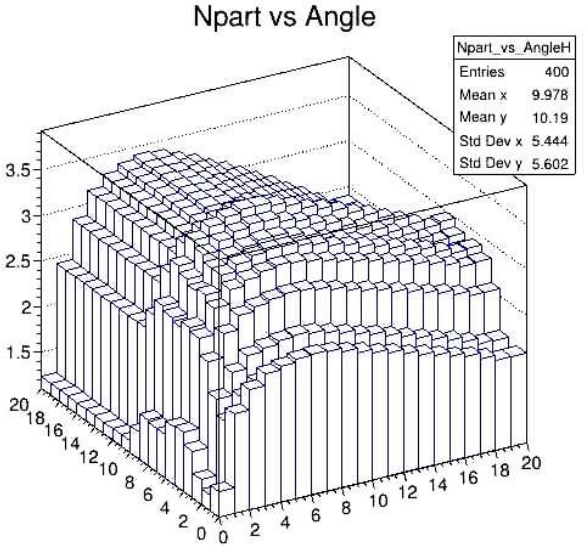

Figure 12. Domains for the number of participants and azimuthal angle difference for twenty bins [Owner-draw].

DOI: 10.54254/2753-8818/28/20230428

Figure 12 was generated by ROOT. Npart refers to the number of participants, while angle refers to the azimuthal angle difference. x and y axis is Npart and angle, while z axis is the average path length difference for each bin and the unit of average path length difference is fm. It shows the domains for the number of participants and the azimuthal angle difference for twenty bins. The value of eccentricity in second harmonic and third harmonics is set to the value in the ninth bin and twentieth bin, with indexes 8 and 19.

5. Discussion

The result of the research was comparatively satisfactory. The program produced a relatively stable outcome at the level of 106. For a lower level, the result started to reveal its variance, which was also anticipated from the Law of Big Numbers. From the result of this experiment, we assumed that the least available number level would be between 105 and 106. That was due to the fact that currently found a minimum of ten bins and twenty bins were both at the same level. However, as precision increases, the required number range should also be increased.

Besides, using the result from the trails at a lower level, we found that the azimuthal angle difference and number of participants would be the most fluctuating independent variables. The eccentricity at the second harmonic fluctuated less, while the eccentricity at the third harmonica didn't fluctuate at all. From here, we assumed that the fluctuation was reciprocal to the importance of asymmetry. This provided us with the conclusion that the eccentricity at the third harmonica deserved to be the most important variable among all factors, while the number of participants and the azimuthal angle difference were affected the least during the collision.

It's noticeable that we expected that the eccentricity of the third harmonicity will be as high as possible to maximize the path length difference. Therefore, it was expectable that the domain for eccentricity of the third harmonica would be closer to 1 as the accuracy was higher. Though there was no accurate evidence showing the tendency of change in angle, we inferred that the increase in accuracy would push the boundary closer to 3.14, which was exactly 180 degrees. This inference might only remain as we were making a collision in two particles who are the identical elements. By having an azimuthal angle difference of 180 degrees, we were making the largest difference.

6. Conclusion

Our research utilized the Glauber Model to simulate the collision process. By analyzing these data, we reached the conclusion that domains for independent variables maximizing the asymmetry were (0.4, 0.5) for eccentricity in the second harmonic, (0.9, 1.0) for eccentricity in the third harmonic, (2.51, 3.14) for azimuthal angle difference, and (125, 166) for the number of participants. For higher precision, we have (0.45, 0.50) for eccentricity in the second harmonic, (0.95, 1.0) for eccentricity in the third harmonic, (2.82, 3.14) for azimuthal angle difference, and (146, 166) for number of participants. There was still plenty of improvement in these studies. In this simulation, we failed to find the minimized sample size for different numbers of bins. Rather, we only gave an ambiguous range for the minimum number of data points. Besides, we failed to find the difference in the minimum number of data points during the simulation, which should take place due to the Law of Big Numbers. In future research, one potential direction would be increasing the sample size at a lower number level to find the exact utilizable situation for the result from our research.

Acknowledgement

Haotian Xu, Ziyan Song, and Junzhe Shi contributed equally to this work and should be considered co-first authors.

References

[1] W. Pauli. (1957). Il Nuovo Cimento 6, 204 . doi:10.1007/BF02827771.
[2] G. Luders (1957). Ann. Phys. 2, 1 . doi:10.1016/0003-4916(57)90032-5

DOI: 10.54254/2753-8818/28/20230428

[3] P. D. C. King, T. D. Veal, P. H. Jefferson, J. Zúñiga Pérez, V. Muñoz Sanjosé, and C. F. McConville. (2009). Unification of the electrical behavior of defects, impurities, and surface states in semiconductors: Virtual gap states in CdO, Phys. Rev. B 79, 035203.

[4] Bonetti, L., dos Santos Filho, L. R., Helayël-Neto, J. A., and Spallicci, A. D. A. M.. (2017). Effective photon mass by Super and Lorentz symmetry breaking, Phys. Lett. B 764, 203–206. arxiv:1607.08786

[5] Glauber, R. J. (1963). Time-dependent statistics of the Ising model. Journal of Mathematical Physics, 4(2), 294–307. https://doi.org/10.1063/1.1703954

[6] M. S. Green. (1954). Markoff random processes and the statistical mechanics of time-dependent phenomena. II. Irreversible processes in fluids, J. Chem. Phys. 22, 398–413.

[7] Arnold, P., Moore, G. D., & Yaffe, L. G. (2001). Photon emission from quark-gluon plasma: Complete leading order results. Journal of High Energy Physics, 009–009. https://doi.org/10.1088/1126-6708/2001/12/009

[8] Sh. Shuzhe, K. Zhou, J. Zhao, S. Mukherjee, and Z P. huang. (2022). Heavy quark potential in the quark-gluon plasma: Deep neural network meets lattice quantum chromodynamics. Physical Review D, 105(1), 014017. doi:10.1103/PhysRevD.105.014017.

[9] Alver, B., Baker, M., Loizides, C., & Steinberg, P. (2008). The phobos glauber monte Carlo. arXiv.org. https://arxiv.org/abs/0805.4411

[10] D. Lafferty and A. Rothkopf. (2019). Quarkonium Phenomenology from a Generalized Gauss Law, Universe, 5(5), 119. doi:10.3390/universe5050119